32–292 K is 0.95, which gives $S = 1.46$, which is higher than the expected value of 1.1 for 2.2 holes per formula in $Tl_{1.8}Re_6Se_{12}$. The reason for this is not yet clear.

The resistivity and magnetic measurement results are as expected. Each rhenium atom is five-coordinated by selenium atoms in a square-pyramidal geometry (dsp^3), which leaves four d orbitals for each rhenium atom. According to molecular orbital calculations for M_6X_8 clusters,[18-20] there are 24 orbitals per cluster, 12 of which are bonding and 12 are antibonding orbitals with a substantial energy gap between. In $Tl_4Re_6X_{12}$, Tl and Re ions are formally in +1 and +3 oxidation states, respectively,[21] while both X and X_2 are in −2 formal oxidation state. There are 24 electrons per cluster unit, which completely fill the bonding states and leave the antibonding states empty. This explains the semiconducting behavior. The magnitude of the energy gap between bonding and antibonding states is determined by the nature of the bridging groups. Since Se 4p orbitals have greater overlapping ability than S 3p orbitals, it is not surprising that the resistivity and the activation energy of the sulfide are much higher than corresponding values of the Se analogue. Since all the electrons are paired, the diamagnetic behavior of $Tl_4Re_6Se_{12}$ seen in Figure 4 is not unexpected. The upturn of the susceptibility at low temperature found for $Tl_4Re_6Se_{12}$ is probably due to the existence of paramagnetic impurities in the sample. In $Tl_{1.8}Re_6Se_{12}$, holes are expected in the valence band and metallic and Pauli paramagnetic behavior would be anticipated. The source of the observed paramagnetic behavior (Figure 4) is not understood at this time. The magnetic data are consistent with the p-type behavior indicated by the room-temperature Seebeck measurement.

Acknowledgment. We are indebted to Dr. Tom Halbert of Exxon Research and Engineering Co., Annandale, NJ 08801, for helping us with X-ray data collection and structure solution. This research was partially supported by the Office of Naval Research, the National Science Foundation—Solid State Program, under Grants DMR-84-04003, DMR-84-08266, DMR-87-14072, and DMR-87-05620.

Registry No. $Tl_4Re_6Se_{12}$, 117201-42-0; TlSe, 12039-52-0; Re, 7440-15-5; Se, 7782-49-2; Tl_2Se, 15572-25-5; $Tl_4Re_6S_{12}$, 117201-37-3; TlS, 12039-09-7; Tl, 7440-28-0; S, 7704-34-9.

Supplementary Material Available: For $Tl_4Re_6Se_{12}$, Tables SI, SIII, and SIV, listing crystal and refinement data, anisotropic thermal parameters, and nonessential bond distances and angles (7 pages); Table SII, listing observed and calculated structure factors (5 pages). Ordering information is given on any current masthead page.

(18) Cotton, F. A.; Haas, T. E. *Inorg. Chem.* **1964**, *3*, 10.
(19) Bursten, B. E.; Cotton, F. A.; Stanley, G. G. *Isr. J. Chem.* **1980**, *19*, 132.
(20) Hughbanks, T. *Inorg. Chem.* **1986**, *25*, 1492.
(21) Huan, G.; Greaney, M.; Greenblatt, M.; Liang, G.; Croft, M. *Solid State Ionics*, in press.

Contribution from the Department of Chemistry, Rutgers, The State University of New Jersey, New Brunswick, New Jersey 08903, Laboratoire de Chimie Theorique, Universite de Paris-Sud, 91405 Orsay, France, and Department of Chemistry, North Carolina State University, Raleigh, North Carolina 27695-8204

Resistivity Anomalies of the Diphosphate Tungsten Bronze $Cs_{1-x}P_8W_8O_{40}$ (x = 0–0.46) and Its Partially Substituted Phases $Cs_xA_yP_8W_8O_{40}$ (A = Rb, Na) and $CsP_8W_{8-x}Mo_xO_{40}$: Synthesis, Physical Property Measurements, and Band Electronic Structure Calculations

Enoch Wang,[†] Martha Greenblatt,*[,†] Idris El-Idrissi Rachidi,[‡] Enric Canadell,*[,‡] and Myung-Hwan Whangbo*[,§]

Received November 8, 1988

The cesium phosphate tungsten bronze $CsP_8W_8O_{40}$ exhibits a resistivity hump at ~160 K and a resistivity upturn at ~24 K. To understand the origin of these anomalies, we prepared cesium-deficient phases, $Cs_{1-x}P_8W_8O_{40}$, and alkali-metal- and molybdenum-substituted phases, $Cs_xA_yP_8W_8O_{40}$ ($x + y > 1$) and $CsP_8W_{8-x}Mo_xO_{40}$, and measured their electrical resistivities and magnetic susceptibilities. Those results are interpreted on the basis of the tight-binding band electronic structures calculated for the W_4O_{18} chain and the $P_8W_8O_{40}$ lattice.

The phosphate tungsten bronze $CsP_8W_8O_{40}$ contains W_4O_{18} chains (**1**) made of corner-sharing WO_6 octahedra.[1] Those chains

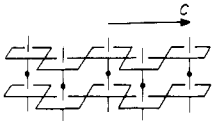

1a

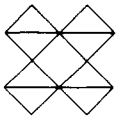

1b

are linked together by P_2O_7 groups (**2**) to form octagonal channels, where Cs atoms reside. The W_4O_{18} chains are isolated in Cs-$P_8W_8O_{40}$, so this bronze is expected to be quasi-one-dimensional in electronic properties. Indeed, the electrical transport and magnetic properties of $CsP_8W_8O_{40}$ are consistent with this picture.[2]

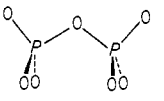

2a

2b

The resistivity versus temperature plot of $CsP_8W_8O_{40}$ shows the presence of two resistivity anomalies at ~160 and ~24 K: it is semiconducting from ~760 to ~160 K, metallic between ~160 and ~24 K, and semiconducting below ~24 K. In order to gain insight into the nature of the resistivity hump at ~160

[†] Rutgers University.
[‡] Universite de Paris-Sud.
[§] North Carolina State University.

(1) Goreaud, M.; Labbe, Ph.; Raveau, B. *J. Solid State Chem.* **1985**, *56*, 41.
(2) Wang, E.; Greenblatt, M. *J. Solid State Chem.* **1988**, *76*, 340.

0020-1669/89/1328-2451$01.50/0

Table I. Parameters and Exponents Used in the Calculations

atom	orbital	H_{ii}, eV	ζ_1	ζ_2	c_1[a]	c_2[a]
O	2s	−32.3	2.275			
	2p	−14.8	2.275			
P	3s	−20.2	1.88			
	3p	−12.5	1.63			
W	5d	−10.37	4.982	2.068	0.6685	0.5424

[a] Contraction coefficients used in the double-ζ expansion.

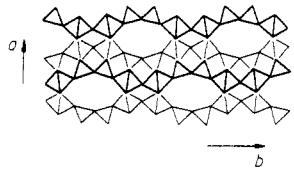

Figure 1. Projection view of the crystal structure of $CsP_8W_8O_{40}$. Cesium atoms (not shown) are present in the octagonal tunnels.

K and the resistivity upturn at ~24 K, we prepared single crystals of the cesium-deficient bronze $Cs_{1-x}P_8W_8O_{40}$ ($x \approx 0.0$–0.46), the partially substituted rubidium and sodium bronzes $Cs_xA_yP_8W_8O_{40}$ (A = Rb, Na), and the molybdenum-substituted bronze $CsP_8W_{8-x}Mo_xO_{40}$ ($x \approx 0.1$–2.1) and measured their physical properties. These results are then interpreted on the basis of band electronic structure calculations on $CsP_8W_8O_{40}$.

Experimental Section

Single crystals of cesium-deficient $Cs_{1-x}P_8W_8O_{40}$ ($x \approx 0.1$–0.5) and partially substituted $Cs_xRb_yP_8W_8O_{40}$ ($x + y > 1$), $Cs_{0.89}Na_{0.17}P_8W_8O_{40}$, and $CsP_8W_{8-x}Mo_xO_{40}$ ($x \approx 0.1$–2.1) bronzes were grown by a solid-state reaction, similar to that described in a recent paper.[2] Appropriate amounts of reagent-grade Rb_2CO_3 and Na_2CO_3 were used in the reaction mixture for the substitution of Cs by Rb and Na, respectively. Single crystals of $CsP_8W_{8-x}Mo_xO_{40}$ were obtained by adding appropriate amounts of Mo metal to decomposition products of a stoichiometric mixture of Cs_2CO_3, $(NH_4)_2HPO_4$, WO_3, and W metal.

The crystals of $Cs_{1-x}P_8W_8O_{40}$, $Cs_xA_yP_8W_8O_{40}$ (A = Rb, Na), and $CsP_8W_{8-x}Mo_xO_{40}$ are golden with a metallic sheen; the crystals form in highly faceted bulky prisms. Samples selected for study had typical dimensions (2–4) × 1 × 0.5 mm^3. Cell parameters were obtained by least-squares analysis of powder data obtained with a Scintag PAD V automated diffractometer employing monochromatic Cu Kα radiation. Silicon was used as an internal standard. The orientation of selected crystals was determined by precession photography.

Electrical resistivity was measured from 2 K to room temperature by using a standard four-probe technique with ultrasonically soldered indium contacts on oriented single crystals. The magnetic susceptibility was measured on a Quantum Design SQUID magnetometer from 2 to 270 K. The Cs stoichiometry in the Cs-deficient crystals was determined on a JEOL 4000 Superprobe electron microprobe with silver-painted electrodes; the uncertainty of Cs content determined is less than 2% by weight. Elemental analyses were obtained on a Beckman plasma emission spectrometer.

Tight-binding band electronic structure calculations[3] were performed on the W_4O_{18} chain (**1**) and also on the $P_8W_8O_{40}$ lattice within the framework of the extended Hückel method.[4] The atomic parameters employed in our work are summarized in Table I.

Crystal Structure

Diagram **1a** shows a perspective view of the W_4O_{18} chain, the projection view of which is given by **1b**. $P_2O_7^{4-}$ ions (**2a**) link those chains by sharing six of the seven oxygen atoms. When each $P_2O_7^{4-}$ ion is represented by **2b**, the crystal structure of $CsP_8W_8O_{40}$ can be shown as in Figure 1. The W_4O_{18} chain is similar in structure to the Mo_4O_{18} chain found in $Li_{0.9}Mo_6O_{17}$[5] but is slightly more tilted due to its linking with the PO_4 tetrahedra of $P_2O_7^{4-}$ ions. With the formal oxidation states Cs^+, O^{2-}, and $P_2O_7^{4-}$, the formal oxidation state of W in $CsP_8W_8O_{40}$ is 4.875. Thus, the electron counting on W is $d^{1.125}$, and there are 4.5 electrons to fill the d-block bands of the W_4O_{18} chain per formula unit (W_4O_{18}).

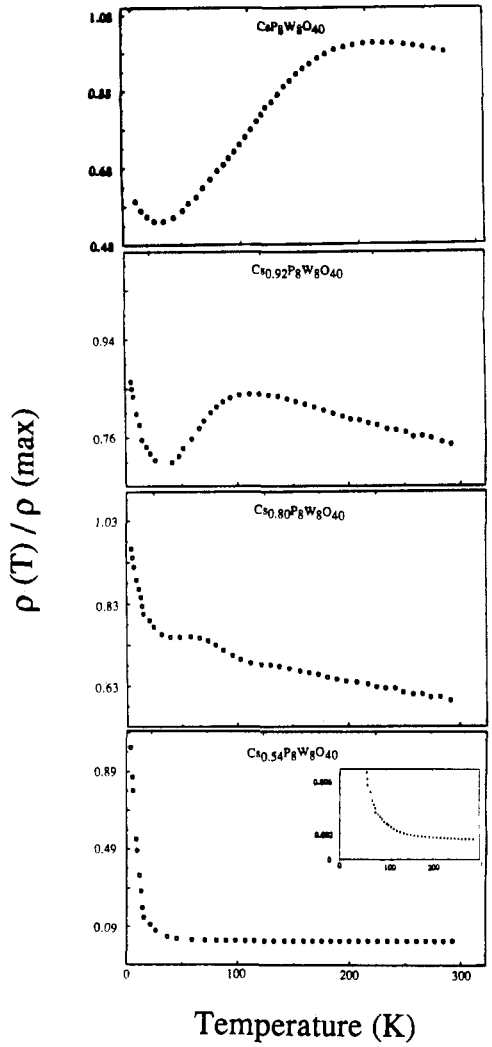

Figure 2. Relative resistivity ($\rho(T)/\rho(\max)$) along the c axis as a function of temperature for single crystals of $Cs_{1-x}P_8W_8O_{40}$.

Table II. Lattice Parameters of Cesium-Deficient $Cs_{1-x}P_8W_8O_{40}$ Phases

sample	a, Å	b, Å	c, Å	V, Å^3
$CsP_8W_8O_{40}$	13.08 (1)	12.33 (1)	5.300 (2)	855.1 (0.4)
$Cs_{0.92}P_8W_8O_{40}$	13.07 (1)	12.33 (1)	5.298 (5)	854.1 (0.4)
$Cs_{0.80}P_8W_8O_{40}$	13.06 (1)	12.34 (1)	5.301 (2)	854.0 (0.6)
$Cs_{0.54}P_8W_8O_{40}$	13.06 (1)	12.33 (1)	5.296 (1)	852.8 (0.3)

Physical Properties

A. $Cs_{1-x}P_8W_8O_{40}$ ($x \approx 0.0$–0.46). The electrical resistivities of $Cs_{1-x}P_8W_8O_{40}$ are summarized in Figure 2. The broad resistivity peak of $CsP_8W_8O_{40}$ at ~160 K is gradually shifted toward lower temperatures, as the Cs content is decreased. At $x = 0.20$ this peak is barely observable, and at $x = 0.46$ only semiconducting behavior is seen in the whole temperature range. The resistivity upturn of $CsP_8W_8O_{40}$ at ~24 K does not seem to be affected significantly by decreasing Cs concentration. Qualitative Seebeck measurements on $CsP_8W_8O_{40}$ showed p-type conductivity at room temperature but n-type conductivity below 100 K.[2]

The temperature variation of the magnetic susceptibility of $CsP_8W_8O_{40}$ is Pauli paramagnetic,[2] indicative of metallic behavior, while that of $Cs_{0.54}P_8W_8O_{40}$ shows paramagnetic behavior found for systems with localized electrons (see Figure 3a).

As shown in Table II, the cell parameters of the Cs-deficient bronzes with decreasing Cs content do not change significantly

(3) Whangbo, M.-H.; Hoffmann, R. *J. Am. Chem. Soc.* **1978**, *100*, 6093.
(4) Hoffmann, R. *J. Chem. Phys.* **1963**, *39*, 1397. A modified Wolfsberg–Helmholz formula was used to calculate the off-diagonal H_{ij} values. See: Ammeter, J. H.; Burgi, H.-B.; Thibeault, J.; Hoffmann, R. *J. Am. Chem. Soc.* **1978**, *100*, 3686.
(5) Onoda, M.; Toriumi, K.; Matsuda, Y.; Sato, H. *J. Solid State Chem.* **1987**, *66*, 163.

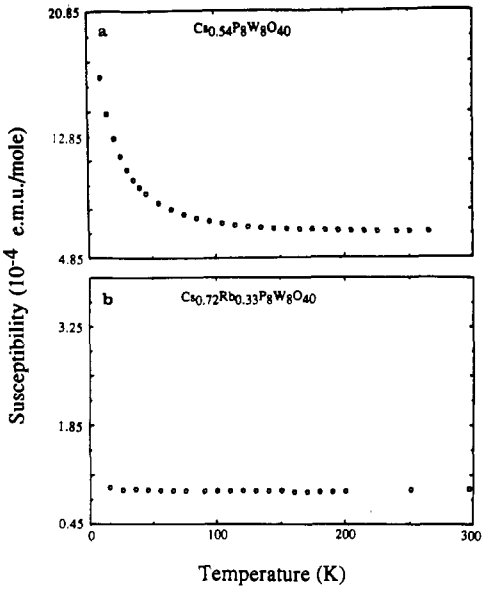

Figure 3. Magnetic susceptibility as a function of temperature for single crystals of (a) $Cs_{0.54}P_8W_8O_{40}$ and (b) $Cs_{0.72}Rb_{0.33}P_8W_8O_{40}$.

Table III. Lattice Parameters of $Cs_xA_yP_8W_8O_{40}$ (A = Rb, Na) Phases

sample	a, Å	b, Å	c, Å	V, Å^3
$CsP_8W_8O_{40}$	13.08 (1)	12.33 (1)	5.300 (2)	855.1 (0.4)
$Cs_{0.97}Rb_{0.16}P_8W_8O_{40}$	13.07 (1)	12.33 (1)	5.303 (2)	854.8 (0.4)
$Cs_{0.89}Rb_{0.21}P_8W_8O_{40}$	13.06 (1)	12.33 (1)	5.305 (3)	854.1 (0.6)
$Cs_{0.72}Rb_{0.33}P_8W_8O_{40}$	13.06 (2)	12.36 (1)	5.301 (4)	855.3 (1.1)
$Cs_{0.89}Na_{0.17}P_8W_8O_{40}$	13.08 (2)	12.34 (1)	5.306 (5)	856.1 (0.8)

compared to those of the host, $CsP_8W_8O_{40}$. This suggests that the observed changes in the broad resistivity peak at ~160 K are electronic rather than structural in origin. The observed systematic decrease in the unit cell volume is consistent with decreasing amounts of Cs in the cavities.

B. $Cs_xA_yP_8W_8O_{40}$ (A = Rb, Na). $Cs_xRb_yP_8W_8O_{40}$ compounds with $x + y > 1$, as determined by chemical analysis, are obtained as a result of attempts to prepare $Cs_{1-x}Rb_xP_8W_8O_{40}$. The absolute resistivity of $Cs_xA_yP_8W_8O_{40}$ is smaller along the c axis than in the ab plane, thereby showing a pseudo-1D character. Figure 4 shows the resistivity determined for oriented single crystals of $Cs_{0.89}Na_{0.17}P_8W_8O_{40}$, $Cs_{0.97}Rb_{0.16}P_8W_8O_{40}$, $Cs_{0.89}Rb_{0.21}P_8W_8O_{40}$, and $Cs_{0.72}Rb_{0.33}P_8W_8O_{40}$. The resistivity hump at ~160 K is absent for measurements along the crystallographic c axis in all the samples. However, a semiconductor-to-metal transition is seen in the resistivity of $Cs_xA_yP_8W_8O_{40}$ when measured in the ab plane, although the transition temperature, T_{sm}, does not scale with $x + y$ and appears to be sample dependent. Rb substitution broadens the metal–insulator transition at ~24 K. This broadening increases with the Rb concentration, regardless of the $x + y$ value. Thus, this may be attributed to the increasing concentration of defects, as observed for the blue bronze $(K_{1-x}Rb_x)_{0.3}MoO_3$[6] and the purple bronze $(Li_{1-x}Na_x)_{0.9}Mo_6O_{17}$.[7]

The magnetic susceptibilities for all $Cs_xRb_yP_8W_8O_{40}$ phases show temperature-independent (i.e. Pauli paramagnetic) behavior, indicative of metallic character. As a representative example, Figure 3b shows the magnetic susceptibility for $Cs_{0.72}Rb_{0.33}P_8W_8O_{40}$. The unit cell parameters of the Na- and Rb-substituted $Cs_xA_yP_8W_8O_{40}$ phases are similar to those of the host (Table III).

C. $CsP_8W_{8-x}Mo_xO_{40}$ ($x \approx 0.1$–2.1). Figure 5 shows the electrical resistivity data of the molybdenum-substituted bronzes $CsP_8W_{8-x}Mo_xO_{40}$. This isoelectronic substitution gradually suppresses the metallic region of $CsP_8W_8O_{40}$ (Figure 2). As the amount of Mo substitution increases to $x = 0.23$, the resulting bronze shows semiconducting behavior. The temperature dependence of the magnetic susceptibility for this sample shows paramagnetic behavior consistent with the resistivity data.

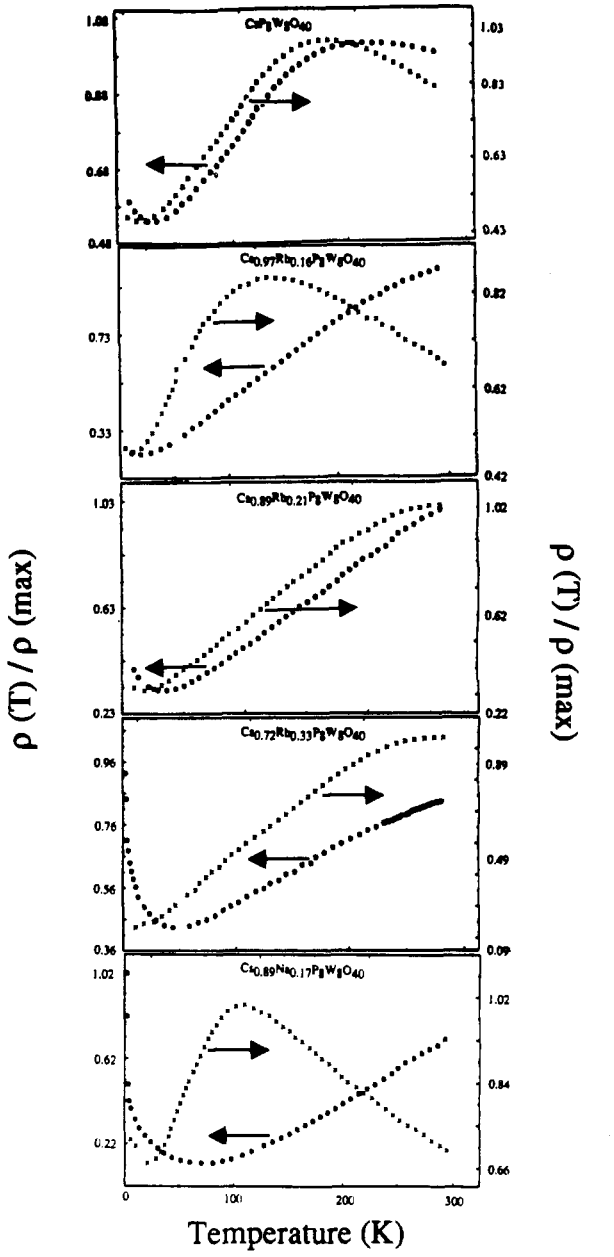

Figure 4. Relative resistivity ($\rho(T)/\rho(\max)$) along the c axis (O) and the ab plane (×) as a function of temperature in single crystals of $Cs_xA_yP_8W_8O_{40}$.

Table IV. Lattice Parameters of Mo-Substituted $CsP_8W_{8-x}Mo_xO_{40}$ Phases

sample	a, Å	b, Å	c, Å	V, Å^3
$CsP_8W_8O_{40}$	13.08 (1)	12.33 (1)	5.300 (2)	855.1 (0.4)
$CsP_8W_{7.99}Mo_{0.01}O_{40}$	13.10 (1)	12.34 (1)	5.298 (3)	856.5 (0.3)
$CsP_8W_{7.84}Mo_{0.16}O_{40}$	13.09 (1)	12.33 (1)	5.300 (6)	855.4 (0.5)
$CsP_8W_{7.77}Mo_{0.23}O_{40}$	13.07 (1)	12.33 (1)	5.306 (3)	855.1 (0.3)
$CsP_8W_{6.83}Mo_{1.17}O_{40}$	13.07 (1)	12.33 (1)	5.296 (2)	853.4 (0.5)
$CsP_8W_{5.9}Mo_{2.1}O_{40}$	13.06 (1)	12.30 (1)	5.291 (5)	850.0 (0.9)

The unit cell dimensions of the $CsP_8W_{8-x}Mo_xO_{40}$ bronzes (Table IV) do not differ much from those of the host $CsP_8W_8O_{40}$ since the effective radius of Mo is comparable with that of W. However, there seems to be a decrease in the cell volume for substantial Mo substitution. Attempts to synthesize the Mo analogue $CsP_8Mo_8O_{40}$ resulted in unidentified multiple phases. Cs–P–Mo–O bronzes could probably be synthesized, but the composition would have to be altered. This possibility was confirmed by the recent report

(6) Schneemeyer, L. F.; DiSalvo, F. J.; Spengler, S. E.; Waszczak, J. V. *Phys. Rev. B: Condens. Matter* **1984**, *30*, 4297.
(7) Ramanujachary, K. V.; Collins, B. R.; Greenblatt, M.; McNally, P.; McCarroll, W. H. *Solid State Ionics* **1986**, *22*, 105.

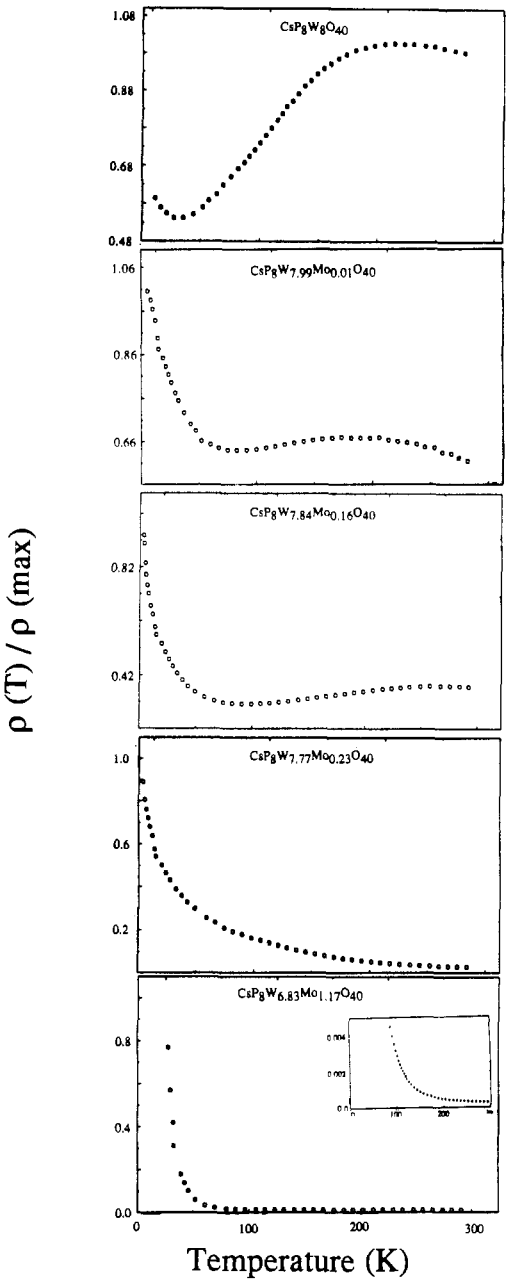

Figure 5. Resistivity along the c axis as a function of temperature for single crystals of $CsP_8W_{8-x}Mo_xO_{40}$.

on the preparation of cesium molybdenum phosphate cluster compounds $Cs_3Mo_5P_6O_{25}$[8] and $Cs_4Mo_8P_{12}O_{52}$.[9]

Band Electronic Structure

The t_{2g}-block bands of the W_4O_{18} chain **1** are shown in Figure 6, where the dashed line represents the Fermi level appropriate for 4.5 d electrons per unit cell. These bands are essentially identical in nature with those of the ideal Mo_4O_{18} chain described in detail elsewhere in connection with $Li_{0.9}Mo_6O_{17}$.[10] Figure 7 shows the t_{2g}-block bands (only the bottom portion) of the $P_8W_8O_{40}^-$ lattice. Since this lattice has two W_4O_{18} chains per unit cell, it has twice as many t_{2g}-block bands as does the W_4O_{18} chain and nine electrons to fill them. Except for the band doubling and a very small splitting in each pair of bands, the t_{2g}-block bands of the $P_8W_8O_{40}^-$ lattice are identical with those of the W_4O_{18} chain.

The most important features of the t_{2g}-block bands in Figures 6 and 7 can be summarized as follows: (a) The Fermi level lies close to, but above, the top of the flat filled bands. (b) The Fermi level lies close to, but below, the bottom of the dispersive, one-dimensional, empty bands. (c) There exist one-fourth-filled one-dimensional bands, which are dispersive. These three characteristics are schematically represented by diagram **3**, where

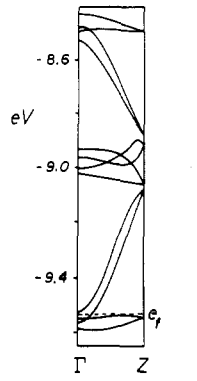

Figure 6. Dispersion relations of the t_{2g}-block bands of the W_4O_{18} chain, where $\Gamma = 0$ and $Z = c^*/2$. The Fermi level (dashed line) is for 4.5 d electrons per formula unit W_4O_{18}.

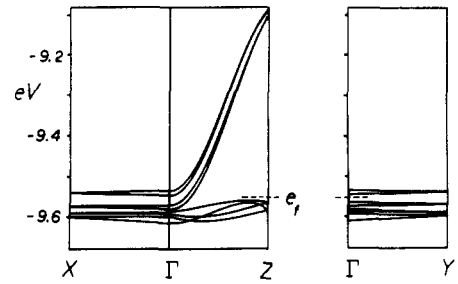

Figure 7. Dispersion relations of the bottom portion of the t_{2g}-block bands calculated for the $P_8W_8O_{40}^-$ lattice, where $\Gamma = (0, 0, 0)$, $X = (a^*/2, 0, 0)$, $Y = (0, b^*/2, 0)$, and $Z = (0, 0, c^*/2)$. The Fermi level is for nine d electrons per unit cell.

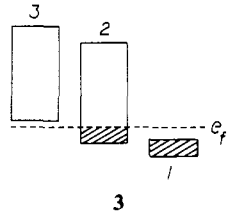

3

bands 2 and 3 refer to the dispersive one-dimensional bands while band 1 refers to the flat bands. In the following, we discuss the electrical properties of $CsP_8W_8O_{40}$ and its substituted analogues on the basis of diagram **3**.

Correlation of Electrical Properties with Band Electronic Structure

A. Resistivity Anomalies of $CsP_8W_8O_{40}$. In understanding the nature of the ~160 K resistivity hump in $CsP_8W_8O_{40}$ (Figure 2), it is necessary to recall that the carriers are holes above 160 K but electrons in the 24–160 K region.[2] In diagram **3** the Fermi level is close to the top of band 1 and also to the bottom of band 3. Thus, with thermal energy, electrons are excited from band 1 to bands 2 and 3. One-dimensional bands have a high density of states at their bottom (and at their top as well). The bottom of band 2 is already filled, while that of band 3 is empty, so that thermal electron excitation into the bottom of band 3 either from band 2 or from band 1 is quite likely.[11] This creates holes in band 1. The hole contribution to conductivity from band 1 is activated since the effective mass of this band is large due to its narrowness. If electrons of band 2 and 3 do not significantly contribute to

(8) Lii, K. H.; Haushalter, R. C.; O'Connor, C. J. *Angew. Chem., Int. Ed. Engl.* **1987**, *26*, 549.
(9) Lii, K. H.; Haushalter, R. C. *J. Solid State Chem.* **1987**, *69*, 320.
(10) Whangbo, M.-H.; Canadell, E. *J. Am. Chem. Soc.* **1988**, *110*, 358.
(11) (a) Pouget, J. P.; Noguera, C.; Moudden, A. H.; Moret, T. *J. Phys. (Les Ulis, Fr.)* **1985**, *46*, 1731. (b) Whangbo, M.-H.; Schneemeyer, L. F. *Inorg. Chem.* **1986**, *25*, 2424.

conductivity due to thermal motions of the lattice, the hole contribution will dominate. As the temperature is lowered below 160 K, deexcitation of electrons from bands 2 and 3 to band 1 will remove the holes of band 1. Further, thermal motions of the lattice are reduced. Thus, electrons of band 2 contribute significantly to conductivity, so that the $CsP_8W_8O_{40}$ bronze is metallic and its carriers are electrons below 160 K. The resistivity upturn at ~24 K can be ascribed to a charge density wave (CDW) associated with the one-fourth filled band 2, since it is a strongly one-dimensional one. It should be possible to observe a CDW with vector $q_{CDW} \approx 0.25c^*$.

B. $Cs_{1-x}P_8W_8O_{40}$. Figure 2 shows that the resistivity hump of $Cs_{1-x}P_8W_8O_{40}$ (at ~160 K for $x = 0$) is gradually shifted to a lower temperature as x increases toward 0.5 and that, at $x \approx 0.5$, the bronze becomes semiconducting at all temperatures. These observations can be explained as follows: as x increases from 0.0 to 0.5, the number of electrons in band 2 decreases from 0.5 to 0.25. As the electron density in band 2 decreases, screening among the electrons of the band is reduced, so that the electrons become more susceptible toward localization around Cs^+-rich neighbors. Therefore, even electrons of band 2 may require activated conductivity. Thus, the resistivity hump of $Cs_{1-x}P_8W_8O_{40}$ is gradually shifted to a lower temperature as the Cs content is decreased, and beyond a certain value of x, the bronze becomes semiconducting.

C. $Cs_xA_yP_8W_8O_{40}$ (A = Rb, Na). Figure 4 shows that, in contrast to $Cs_{1-x}P_8W_8O_{40}$, the $Cs_xA_yP_8W_8O_{40}$ bronze does not have a resistivity hump when measured along the c crystallographic direction. For the partially substituted bronze, $x + y > 1$, so that it has more d electrons than does $CsP_8W_8O_{40}$. In diagram 3, which is applicable for $x + y = 1$, thermal excitation probability is large for the excitation to the bottom of band 3, as already mentioned. Thus, provided that the $x + y$ value of the Rb- and Na-substituted bronze is large enough to fill the bottom portion of band 3, thermal excitation from band 1 would be weak. Then the hole contribution to conductivity from band 1 is diminished so that electron contribution from band 2 becomes dominant. As a result, the resistivity hump along the c axis found for $Cs_{1-x}P_8W_8O_{40}$ will be absent in $Cs_xA_yP_8W_8O_{40}$ ($x + y > 1$). The sample-dependent semiconductor-to-metal transition seen in the resistivity of $Cs_xA_yP_8W_8O_{40}$ samples in the ab plane cannot be accounted for in terms of the band diagram, and its origin is not clear.

D. $CsP_8W_{8-x}Mo_xO_{40}$. According to Figure 5, the metallic character of $CsP_8W_8O_{40}$ quickly disappears when a small amount of W is substituted with Mo. This result is expected since the random distribution of Mo atoms in the W_4O_{18} chains will disrupt the band electron contribution to conductivity.

Concluding Remarks

$CsP_8W_8O_{40}$ exhibits a broad resistivity hump at ~160 K and a resistivity upturn at ~24 K. To examine the origin of these resistivity anomalies, we prepared its electron-deficient and electron-rich analogues ($Cs_{1-x}P_8W_8O_{40}$ and $Cs_xA_yP_8W_8O_{40}$ ($x + y > 1$), respectively), measured their physical properties, and performed tight-binding band electronic structure calculations on the $P_8W_8O_{40}^-$ lattice. The present work suggests the ~160 K resistivity hump to be due to the fact that the Fermi level of the $P_8W_8O_{40}^-$ lattice, which occurs near the bottom of dispersive one-dimensional bands, lies very close to the top of flat, filled bands and also very close to the bottom of dispersive, one-dimensional, empty bands. Our study also suggests that the resistivity upturn of Cs at ~24 K stems from a CDW associated with the dispersive one-dimensional bands.

Acknowledgment. We thank Dr. J. S. Delaney for the electron microprobe analysis of Cs in the samples. Work at Rutgers University was supported by the National Science Foundation-Solid State Chemistry Grants DMR-84-04003 and DMR-87-14072 and the National Science Foundation Materials Research Instrumentation Grants DMR-84-08266 and DMR-87-05620. Work at the Universite de Paris-Sud and North Carolina State University was supported by NATO, Scientific Affairs Division, and also by DOE, Office of Basic Sciences, Division of Materials Science, under Grant DE-FG05-86ER45259.

Contribution from the Laboratoire de Chimie Theorique, Universite de Paris-Sud, 91405 Orsay, France, and Departments of Chemistry, Rutgers, The State University of New Jersey, New Brunswick, New Jersey 08903, and North Carolina State University, Raleigh, North Carolina 27695-8204

Structural and Electronic Origin of the Three-Dimensional Electrical Properties of $P_8W_{12}O_{52}$ and Its Inserted and Substituted Analogues $A_xP_8W_{12}O_{52}$ (A = Li, Na) and $P_8W_{12-x}Mo_xO_{52}$

Enric Canadell,*[†] Idris El-Idrissi Rachidi,[†] Enoch Wang,[‡] Martha Greenblatt,*[‡] and Myung-Hwan Whangbo*[§]

Received November 21, 1988

Single crystals of $P_8W_{12}O_{52}$ and its inserted and substituted analogues $A_xP_8W_{12}O_{52}$ (A = Li, $x = 0.16$; A = Na, $x = 0.22$) and $P_8W_{12-x}Mo_xO_{52}$ ($x = 0.28, 0.40, 0.68$) were prepared, and their electrical resistivities and magnetic susceptibilities were measured. All of these bronzes are found to be isotropic metals. Our tight-binding band electronic structure calculations on $P_8W_{12}O_{52}$ show that the three-dimensional metallic character originates from a three-dimensional linking of WO_6 octahedra in the lattice and the relatively high oxidation state of W. Examination of the structural relationship between $P_8W_{12}O_{52}$ and $CsP_8W_8O_{40}$ led to a new synthetic route for the preparation of $CsP_8W_8O_{40}$ from $P_8W_{12}O_{52}$. With use of this new method, $Tl_2P_8W_8O_{40}$ (isostructural with $CsP_8W_8O_{40}$) was synthesized for the first time.

Introduction

Tungsten bronzes of the diphosphate ions $P_2O_7^{4-}$ have open framework channel structures, in which alkali-metal and other metal ions can be intercalated. So far, three types of channel structures have been identified in diphosphate tungsten bronzes: $CsP_8W_8O_{40}$ has octagonal channels,[1] a family of $A_x(P_2O_4)_4(WO_3)_{4m}$ (A = K with $m = 5-11$;[2] A = Rb with $m = 4-11$;[3] A = Tl with $m = 8$;[4] A = Ba with $m = 6-10$[5]) has hexagonal

[†] Universite de Paris-Sud.
[‡] Rutgers University.
[§] North Carolina State University.

(1) Goreaud, M.; Labbe, Ph.; Raveau, B. *J. Solid State Chem.* **1985**, *56*, 41.
(2) Hervieu, M.; Raveau, B. *J. Solid State Chem.* **1982**, *43*, 291.
(3) Giroult, J. P.; Goreaud, M.; Labbe, Ph.; Raveau, B. *Acta Crystallogr.* **1982**, *B38*, 2342.

0020-1669/89/1328-2455$01.50/0